CrystEngComm

Accepted Manuscript

ROYAL SOCIETY OF CHEMISTRY

www.rsc.org/crystengcomm

Abstract:

In view of high rate fabrication of coated conductors at low-cost, $YBa_2Cu_3O_7$ (YBCO) films on $Ce_{0.9}La_{0.1}O_2$ buffered yttria-stabilized zirconia substrates were deposited by means of a novel low-fluorine metalorganic solution route. A high critical current density of 3 MA/cm^2 (77 K, self field) is achieved on such an all-chemical derived configuration. Structural characterizations show that the enhanced superconductivity performance in the YBCO films is mainly related to the defects induced by the interface.

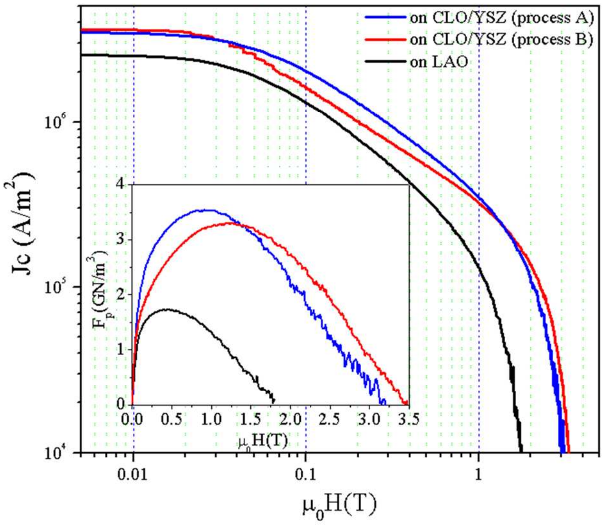

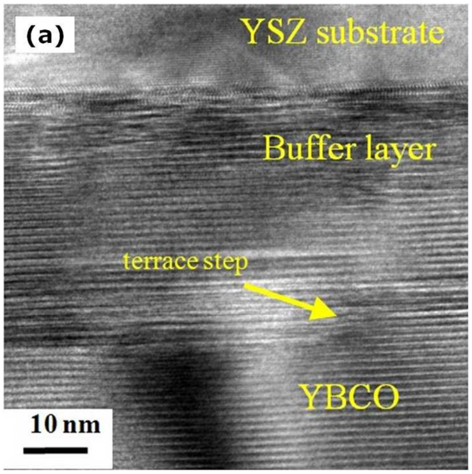

Epitaxial growth of $YBa_2Cu_3O_{7-x}$ films on $Ce_{0.9}La_{0.1}O_{2-y}$ buffered yttria-stabilized zirconia substrates by all-chemical-solution route

Yue Zhao,*[a] Wei Wu,[a,b] Xiao Tang,[a] Niels Hessel Andersen,[c] Zhenghe Han,[b] and Jean-Claude Grivel[b]

Received (in XXX, XXX) Xth XXXXXXXXX 20XX, Accepted Xth XXXXXXXXX 20XX
DOI: 10.1039/b000000x

In view of high rate fabrication of coated conductors at low-cost, $YBa_2Cu_3O_7$ (YBCO) films on $Ce_{0.9}La_{0.1}O_{2-y}$ buffered yttria-stabilized zirconia substrates were deposited by means of a novel low-fluorine metalorganic solution route. A high critical current density of 3 MA/cm^2 (77 K, self field) is achieved on such an all-chemical derived configuration. Structural characterizations show that the enhanced superconductivity performance in the YBCO films is mainly related to the defects induced by the interface.

Manufacturing long-length coated conductors (CCs) with multilayer structures have been demonstrated by several groups or companies using various film deposition techniques [1, 2, 3]. Among these techniques, chemical solution deposition (CSD) routes have attracted most attention. That is not only because it is a cost-effective method with a high potential for large area film deposition, but also due to the nucleation and growth behavior which might generate unique microstructures leading to novel functionalities [4]. Rather extensive studies on applying the CSD technology for either buffer layers or superconducting layers have been carried out worldwide. Nevertheless, concerning high performance CCs tapes manufactured by the so-called all-CSD route (i.e., both the superconducting layer and the buffer layers are deposited by CSD route), only few reports have been published so far [5], implying a limited comprehensive understanding on several key issues, such as solution chemistry, interfacial interactions and defect control. Therefore, great efforts are still needed to further understand the CSD routes used for growth of oxide films in CCs' architecture.

In this work, we focused on establishing the all-CSD processed processed architecture YBCO/$Ce_{0.9}La_{0.1}O_{2-y}$ on single crystal yttria-stabilized zirconia (YSZ) substrates. $Ce_{0.9}La_{0.1}O_{2-y}$ (CLO) films which has shown good compatibility with $YBa_2Cu_3O_7$ (YBCO) grown by pulsed laser deposition in our previous study[6], were chosen as cap layer. A low-fluorine metalorganic solution was proposed for depositing YBCO layers, by which method both a short pyrolysis process and a minimal amount of HF release during heat treatment could be achieved. Particularly, we paid attention on applying relatively low sintering temperature for YBCO films, in order to easily transfer this process to technical substrates with similar buffer layer architecture. Both the structure and superconducting performance of the YBCO/CLO/YSZ stack and an YBCO/ $LaAlO_3$ single crystal as reference were investigated in detail.

The CLO cap layers were prepared by the propionate-based metal-organic solution deposition (MOD) route which has been reported previously [7, 8]. With optimized coating and heat treatment conditions, high quality films with about 20 nm thickness were prepared and used for further YBCO deposition. The low-fluorine MOD solution for YBCO films was prepared as follows. First, a solution (referred to as *solution A*) was made by dissolving home-made yttrium and barium trifluoroacetates in methanol with a Y/Ba ratio of ½, similarly to typical TFA-MOD processes [9]. Secondly, copper acetate was dissolved in a small amount of acrylic acid (10% excess) and de-ionized water. After full reaction and removal of the residual solvent and by-products by vacuum evaporation, a dry copper-based powder was obtained. The final precursor solution was made by mixing the stoichiometic *solution A* and the copper-based powder at room temperature. The total cation concentration was adjusted to 1.5 M by controlling the amount of methanol. The precursor solution was deposited on the CLO buffered YSZ substrates by spin-coating with a speed of 3000 rpm. The heat treatment procedure, including pyrolysis, sintering and oxygenation, used for obtaining superconducting YBCO films was as follows. The pyrolysis process started from 150°C to 400 °C with a ramp of 1.7 °C/min in humid oxygen with a dew point (D.P.) of 20 °C. Then two types of sintering processes were employed for comparison. One is single-step sintering (designated as *process A*), i.e., the pyrolyzed films were directly sintered at 740 °C for 2 hours. For comparison, another process, which is a two-step sintering process (designated as *process B*), was also studied. In this case, the pyrolyzed films were firstly heated to 740 °C for 20 min, prior to annealing at 770 °C for 90 min. Both sintering processes were performed in a humid flow (D.P.=20 °C, with 100 ppm oxygen). The oxygenation was carried out at 450 °C for 3 hours in flowing oxygen gas.

Phase and crystallographic textures were investigated by means of x-ray diffraction (XRD) using Cu K_α radiation in a Bruker D8 four-circle diffractometer. The surface morphology of the films was observed by scanning electron microscopy (SEM, Supra 35) equipped with an inlens detector, while transmission electron microscopy (TEM) observations on the sample cross-section were performed using a Tecnai G2 F20 S-Twin operating at 200 kV. The superconducting performance of the films was characterized by a CRYOGENICH CFMS magnetometer. The superconducting transition temperature (T_c) was determined by AC susceptibility measurements with an AC field amplitude of 0.1 mT and frequency of 21 Hz. The critical current densities, J_c, were determined by vibrating sample measurements (VSM, Cryogenic) and calculated based on the Bean model [10] using the opening of the hysteresis loops obtained under magnetic field applied perpendicular to the plane of the films.

As shown in Fig. 1a), a representative *θ-2θ* XRD scan pattern collected from YBCO/CLO/YSZ made by *process A* suggests that the film was completely converted without any impurities other than $BaCeO_3$ and secondary texture components. The (103) pole figure measured on the film surface shows a highly epitaxial texture, being indicative of the YBCO growth throughout the film thickness. The homogeneous microstructure without randomly orientated grains in the YBCO film is also confirmed by SEM, as shown in Fig.1 (b). There is little difference between all the three films by means of conventional *θ-2θ* XRD analysis or SEM observations. More details about the quantitative structural analysis of the films can be found in Table 1. The YBCO/LAO sample exhibits slightly sharper in-plane and the out-of-plane textures relative to those grown on CLO/YSZ substrates. The similarity of the texture quality of the YBCO films deposited on CLO/YSZ substrates implies that the texture is mainly determined by the quality of substrate, rather than the heat treatment used in this study. The intensity ratios of the (005) and (004) reflections, which is smaller than 20 also suggests that the oxygen deficiency, δ, is smaller than 0.1 in all these three films. Regarding superconducting performance, all these YBCO films exhibit a superconducting transition temperature above 89 K. The higher T_c (about 2 K difference compared to *process A*) observed on the sample made by *process B* could be explained by the improved crystal quality forming at relatively high growth temperature in such two-step sintering processes. It is believed that due to the lower sintering temperature used in *process A*, the degree of disorder between Y and Ba atoms in the structure is higher, compared with that made by process A, which would lead to the T_c difference [11]. The broader transitions for both films grown on CLO/YSZ could be attributed to either the strain effect or the deterioration of the texture quality from the interface. The $J_c(H)$ dependence at 77 K of all the films shows a similar behavior as seen in Fig.2. The J_c in log–log scale exhibits a plateau at low fields (up to the accommodation field, B*, determined by the criterion $J_c(B^*)/J_c(0)=0.9$.), which is associated with a single-pinning regime, while a power-law dependence $J_c(H) \propto H^{-\alpha}$,corresponding to a collective interacting regime of vortices, is observed in the field range between the end of the low-field plateau and the high-field limit where J_c decrease rapidly due to the presence of flux creep. Several characteristics extracted from these curves are listed in Table 1 as well. The films deposited on CLO/YSZ exhibit higher J_c values in the whole field range and weaker field dependence, which is also reflected by the larger pinning force F_p ($F_p=B\times J_c$) and higher value of the accommodation fields B* at 77 K. A large amount of defects is present at the YBCO/CLO interface as illustrated in the TEM pictures shown in Fig. 3. The slightly enhanced J_c(H) at fields between B* and 1.5 T in the sample made by *process A* is probably associated with low growth-temperature induced structural defects, which could act as weak-pinning centers [12]. Using a two-step sintering process is intended to minimize the YBCO-CLO reactivity at relatively low growth temperature, prior to higher temperature annealing to further improve the crystallinity of the YBCO film [13]. This seems in agreement with our results, where a higher T_c on the sample made by *process B* is observed in our study. Further investigations are still needed to interpret the nucleation and growth behaviors of the YBCO films obtained by *process B*.

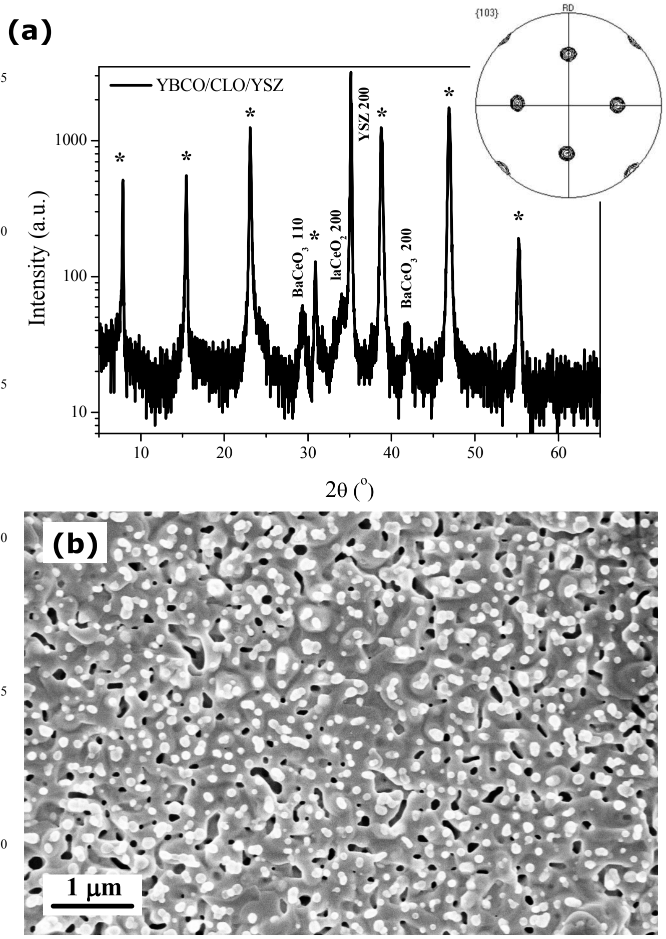

Fig.1. a) *θ-2θ* scan for a 200 nm thick YBCO film grown on a CLO/YSZ substrate with a 20 nm thick CLO layer by *process A* (the peaks marked by asterisks are *00l* reflections of YBCO), and the inset is the YBCO (103) pole figure extracted from electron backscattering diffraction measurements, b) SEM image of the same sample.

In order to shed light on microstructural features on the all-chemical-solution derived structure, we choose the sample made by *process A* for a detailed TEM investigation. In the overview cross-sectional TEM image (Figure 3 a), we observed that the YBCO grows along the c-axis, the [001] direction, onto a 20 nm thick CLO buffer layer with clear boundaries between the YBCO film and the YSZ substrate. We also observed two atomically flat facets joining at a terrace step of 2~3 nm height at the YBCO-buffer layer interface. This is probably a feature inherited from the un-reacted CLO layer. Combining the XRD data and TEM cross-section analysis, it comes out that the thin CLO layer deposited initially reacted to some extent during YBCO layer processing. The main products of the interfacial reaction are Y_2BaCuO_5, $BaCeO_3$ and CuO, and the extent of the reaction is strongly dependent on the sintering process of the YBCO film [14]. A detailed analysis of the YBCO/CLO interface reveals a slight tilt of about 2.5° between the reacted buffer layer and the

Table 1. Summary of quantitative structural analysis and superconductivity performance on the YBCO films

sample	YBCO/LAO (ref. , Process B)	YBCO/CLO/YSZ	
		Process A	Process B
(103) □-scan FWHM (^{o})	1.5	2.4	2.8
(005) rocking curve FWHM (^{o})	0.7	1.5	1.2
I(005)/I(004)	15.7	11.28	12
T_c (K)	91.3	89.4	91.5
Δ T_c (K)	2.6	3.7	4.0
B^*(mT, at 77 K)	25	30	28
α (at 77 K)	-0.90	-0.67	-0.76
F^{MAX}(GN/m^3)	1.7	3.3	3.5
J_c (MA/cm^2, at 77 K, 0 T)	2.5	3.5	3.6

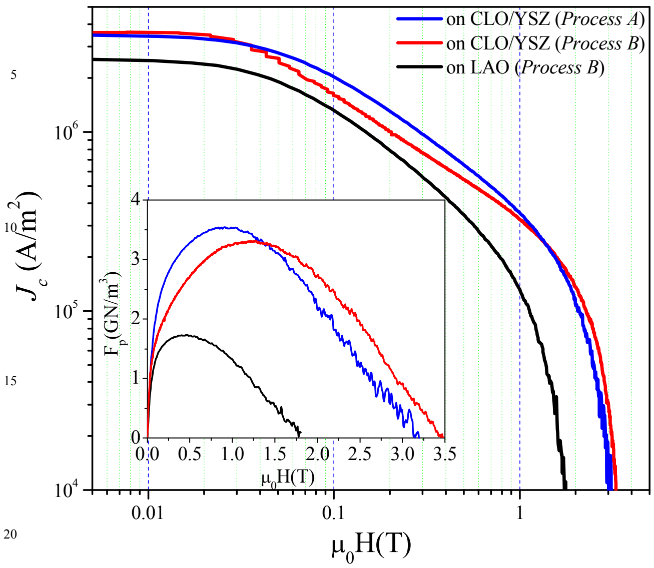

Fig. 2. Double logarithmic plots of J_c vs. magnetic field B measured at 77 K for the YBCO/CLO/YSZ films and the reference sample. Inset: the flux pinning force curves for all three films at 77 K.

YBCO structure as shown in the TEM and Fast Fourier Transform (FFT) images (shown in Fig 3 b), which is probably due to the spiral growth mechanism initiated at the terrace steps on the CLO surface, or due to the slightly misoriented CLO grains at the surface where YBCO nucleates. This observation is also in agreement with TEM observation adn the deterioration of the out-of-plane texture of the films on the buffered YSZ compared to that on the LAO substrate. Without considering the layer interactions, the lattice constant of the CLO buffer layer perfectly matches that of the basal plane of YBCO. Our previous study showed that the interfacial reaction in similar samples occurs as early as 700 ^{o}C [15], which is much earlier than in the other CeO$_2$ cap layers made by physical deposition techniques (i.e., sputtering or PLD) [16, 17]. Additionally, as the layer is only 20 nm thick, it is likely that the strain originating from the

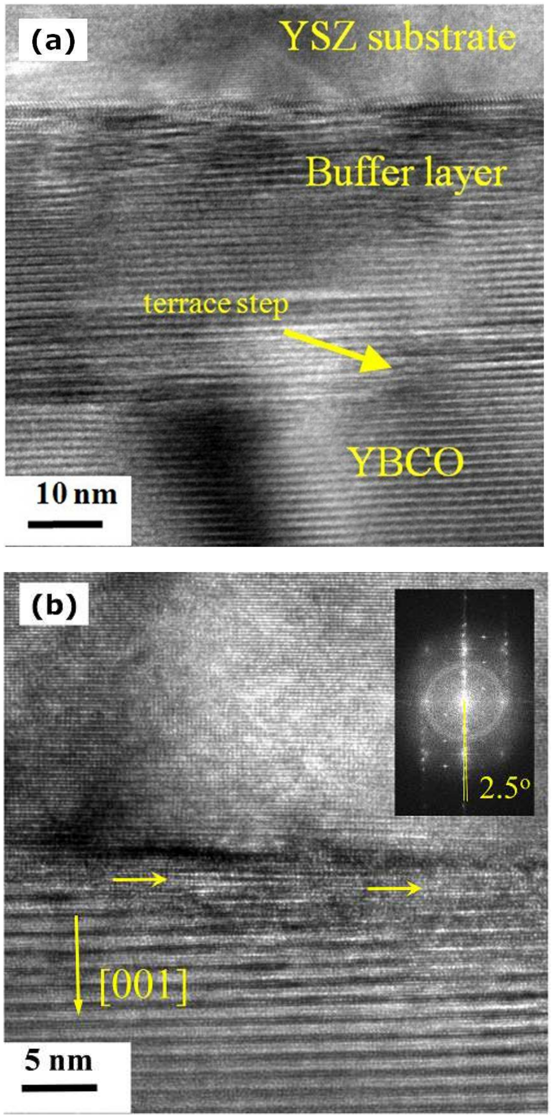

Fig.3. TEM image of a cross-section of a YBCO/CLO/YSZ stack (*process A*), showing a) an overview of the multilayer structure, b)

the YBCO-CLO interface, where the arrows show the dislocated region, and the inset is the FFT image.

CLO/YSZ interface (with a mismatch of about 5%) is transferred to the YBCO/buffer layer interface. Therefore, the 2-5 nm thick dislocation regions and the slight off-axis growth are also partly connected to the large mismatch between the YBCO and the by-products resulting from the interfacial reaction. Even though much stronger pinning forces have been achieved in YBCO films by nanoparticle additions realized by in-situ or ex-situ routes [17, 18], one important issue addressed in the present study is that the low-fluorine metalorganic solution route with good compatibility with the CSD-CLO buffer layer is able to yield promising critical current densities at relatively low growth temperatures which are beneficial to industrialization.

Conclusions

In this work, we have demonstrated the feasibility of using low-fluorine metalorganic solution routes to fabricate YBCO films on CLO buffered YSZ substrates. The results show that a promising critical current density as high as 3 MA/cm^2 (77 K, self field) and a large flux pinning force value of about 3.5 GN/m^3 are achieved under fast pyrolysis and optimized sintering processes. TEM cross-sectional imaging shows that almost all of the CLO buffer layer is consumed by the interfacial reaction during YBCO growth even at low temperature. There are large amounts of dislocations that can act as pinning defects at the interface and are believed to be responsible for the enhanced J_c(H) performance.

Acknowledgement

We thank useful discussion with Dr. Xiaofen Li from University of Houston and some of the XRD analysis assisted by Prof. P. Paturi from University of Turku.

Notes and references

[a] *Address, Department of Energy Conversion and Storage, Technical University of Denmark, 4000Roskilde, Denmark.*
[b] *Address, Department of Physics, Tsinghua University, 100084Beijing, People's Republic of China*
[c] *Address, Department of Physics, Technical University of Denmark, 2800Lyngby, Denmark*

1 Y. Shiohara, N. Fujiwara, H. Hayashi, et al., *Phys. C*, 2009, **469**, 863–867.
2 M.W. Rupich, X. Li, C. Thieme, et al., *Supercond. Sci. Technol.*, 2010, **23**, 014015.
3 V. Selvamanickam, Y. Chen, T. Shi, et al., *Supercond. Sci. Technol*., 2013, **26**, 035006.
4 R. W. Schwartz, T. Schneller and R. Waser, *C. R. Chim*., 2004, **7**, 433-461.
5 M. Bäcker, All-solution Coated Conductors for energy applications [Online]. available at:http://d-nano.com/en/news/events.html
6 Y. Zhao, X.-F. Li, A. Khoryushin, et.al., *Supercond. Sci. Technol.*, 2012, **25**, 015008.
7 Y. Zhao, J.-C. Grivel, A. B. Abrahamsen, et.al., *Mater. Lett.*, 2011, **65**, 2669–2672.
8 Y. Zhao, J.-C. Grivel, A B Abrahamsen, et.al., *IEEE Trans. Appl. Supercond*. 2011, **21**, 2912-2915.
9 Gupta, R. Jagannathan, E. I. Cooper, et.al., *Appl. Phys. Lett.* 1988, **52**, 2077-2079.
10 E. M. Gyorgy, R. B. Vandover, K. A. Jackson, et.al., *Appl. Phys. Lett.*, 1989, 55 283–285
11 J. Ye and K. Nakamura, Phys. Rev. B, 1994, 50, 7099-7106
12 Z. Chen, F. Kametani, S. I.Kim, et.al., *J. Appl. Phys*. 2008, **103**, 043913.
13 K. Zalamova "Fast growth rate of superconducting coated conductors based on metal-organic chemical solutions"Ph. D. Thesis. U. A. Barcelona-ICMAB, Spain, 2009, p 5-145.
14 Boikov Yu A, Claeson T, Erts D, Bridges F and Kvitky Z *Phys. Rev. B,* 1997, **56**, 11312.
15 Y. Zhao, X. Tang, W Wu, J.-C. Grivel. accepted by *Journal of Physics: Conference Series*
16 M S Bhuiyan, M Paranthaman, S Sathyamurthy et, al. *Supercond. Sci. Technol.*, 2003, **16,** 1305–1309.
17 I. Nagino, K. Matsumoto. H. Adachi, et.al., *Physica C,* 2010, **20,** 1308 - 1312.
18 B. Maiorov, S.A.Baily, H. Zhou, O. Ugurlu, et.al., *Nature Materials*, 2009, **8,** 398 - 404.
19 J. Gutierrez, A. Llordes, J. Gazquez, et.al., *Nature Materials*, 2007, **6,** 367 - 373.